AD630286

TT66-60818

TRANSLATION

CAVITATION ON SURFACE IRREGULARITIES OF
TRIANGULAR PROFILE

By

K. K. Shal'nev

FOREIGN TECHNOLOGY

DIVISION

AIR FORCE SYSTEMS COMMAND

WRIGHT-PATTERSON AIR FORCE BASE

OHIO

DDC

APR 4 1966

RECEIVED

DDC-IRA B
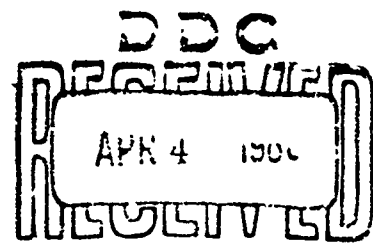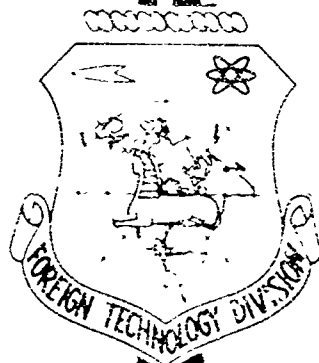
3.60 0.50 33 as

Code 1

UNEDITED ROUGH DRAFT TRANSLATION

CAVITATION ON SURFACE IRREGULARITIES OF
TRIANGULAR PROFILE

BY: K. K. Shal'nev

English pages: 31

SOURCE: Zhurnal Prikladnoy Mekhaniki i Tekhnicheskoy
Fiziki, No. 6, 1962, pp. 68-80.

S/0207-062-000-006   TP5002608

CAVITATION ON SURFACE IRREGULARITIES
OF TRIANGULAR PROFILE

K. K. Shal'nev

(Moscow)

Introduction. Cavitation on surface irregularities, as a cause of intense erosion, have attracted attention when examining the cavitation distruction of screw propellers [1]. A great deal of significance was given to surface irregularities in the onset of cavitation and erosion in turbines by Viderg in his discussion on the report by Dahl [2]. Here also was expressed the fear that a material subject to corrosion will also be unstable against cavitation erosion since pitting due to corrosion may exibit its own form of inducers of cavitation and hence erosion. Later erosion behind surface irregularities were detected repeatedly in Capaln turbines, beyond irregularities due to misalignment of the joints of the wheel chambers [3]. beyond irregularities due to uncleaned finishing of parts at the lathes [4]. etc. Erosion behind surface irregularities was observed under laboratory conditions by Schröter [5].

Schöter produced irregularities on a surface of lead by scratching lines approximately 0.25 mm in width and by boaring circular openings with a diameter of about 0.75 mm. Then the samples — lead

plates — were tested in the diffusion work chamber of a cavitation
tube. When irregularities were located in the zone of intense erosion
effect then both the surface irregularity and nearby portions of the
surface became continuously covered with erosion pitting. If the
irregularities were located at the edge of the cavitation zone
erosion pitting was noted only on surfaces located down stream. It
was clear that only in this case was the irregularity itself the cause
of local cavitation and erosion. In other experiments with lead and
Bakelite Schröter determined the effect of the shape and dimensions
of the irregularities on the time of appearance and onset of erosion.
The irregularities had the form of circular holes and groves. Large
holes with a diameter of 3 mm had no effect on the time of onset of
erosion as compared with the time of onset of erosion for smooth
surfaces. Fine holes with a diameter of 0.75 mm and intersecting
groves shortened the period of onset of erosion by 2 — 4 times.

Thus, if during the preparation of a hydromachine when surfaces
are not easily accessable for mechanical working and also when
irregularities are formed during mounting of the machine they may be
the cause of local cavitation and erosion. Hence it is clear how
important it is to know the conditions of excitation of cavitation
by surface irregularities as a function of their form, size, the
rate of flow and the pressure in the flow.

In previous articles [6, 7] the author has described the results
of studies on cavitation behind models of individual irregularities
carried out in a hydrodynamic tube. At that time models of various
profiles were tested to determine the critical values of the
coefficient of cavitation. Cavitation coefficients were referred to
the average velocity in the cross section of the work chamber of the

FTD-TT-65-1606/1+2+4

hydrodynamic tube with the assumption that the peaks of the
irregularities project beyond the boundary layer. A thought was
expressed concerning the need of taking into account the effect of
the boundary on the magnitude of the critical values of the
coefficients of cavitation.

According to information from Holl. [8], Calehuff and Wislicenus
[9] and then Walker [10] studies were made of cavitation of various
irregularities where upon the author studies the latter by cavitation
behind a model irregularity in the form of a segment of a circle.
Holl [8] studied the conditions of cavitation formation by a surface
irregularity of triangular and segmented profile on isolated models
as well. Finally, Colgate [11] carried out experiments with a mold
of a surface irregularity of the Grand Coulee Spillway Dam which
was destroyed by cavitation.

Below are described the results of new experiments with geometri-
cally similar models of the same triangular profile placed in a wide
range of velocities and with a larger number of models than was
possible in previous studies.

Nomenclature

a — channel height of the working chamber;

l_1 — distance from peak of irregularity to the forward end of the cavitation zone;

l_2 — ditto to the trailing end;

N — disruptor or cavern frequency;

n — index for p, v, q;

p_1 — pressure at nozzle inlet at point M_1;

p_2 — pressure at nozzle outlet at point M_2;

p_3 — pressure at inlet to working chamber at point M_3;

p_4 — pressure at the measurement cross section at point M_4 in the absence of a model;

b — channel width;

a_e — thickness of compressed stream beyond the irregularity in the absence of cavitation;

a_r — irregularity height;

a_e — thickness of cavitation zone;

α — coefficient of compression of the flow of the disruption zone beyond the irregularity and irregularity model;

α_1 — coefficient of compression of the flow beyond the irregularity model;

α_2 — coefficient of compression of the stream beyond the irregularity in the absence of cavitation;

p_e — pressure at the forward special point on the longitudinal flow access;

p_v — water vapor pressure;

p_∞ — pressure at infinity taken equal to the pressure in the measurement cross section in the absence of an irregularity model;

P — coefficient of pressure;

q_n — velocity head;

R^n — Reynolds number for model of surface irregularity;

S — Strouhal number;

v — average cross sectional velocity;

v_0 — velocity along flow axis in front of the irregularity models;

v_s — average velocity in the compression cross section;

u — velocity in the boundary layer at a distance $y \leq 1.0$ mm from the wall;

u_r — velocity at the level of the irregularity peak;

u_{rs} — velocity at the level of the irregularity peak taking into account compression;

y — ordinate of the velocity curve in the measurement cross section calculated from the wall;

α_e — coefficient of compression of flow of zone cavitation;

α_{er} — coefficient of compression of the flow of the zone cavitation and irregularity;

γ — weight of unit volume of water;

ζ — coefficient of resistance;

K — theoretical value of κ corresponding to the onset of cavitation;

κ_0 — coefficinet of cavitation;

$\kappa^{\bullet}$ — value of κ corresponding to the onset of cavitation with reduction in pressure in the range of probable appearance of cavitation;

$\kappa^{\bullet}$ — value of κ corresponding to suppressed cavitation with an increase in pressure in the flow surrounding the cavitation zone;

κ_{el} — coefficient of slot cavitation;

κ_{pr} — coefficient of cavitation of a model of wing profile;

κ_r — coefficient of cavitation of surface irregularity;

$\lambda_{1,2}$ — relative length of expansion of the cavitation zone;

ν — coefficient of kinetic viscosity;

6×25 — arbitrary designation of the experiment variant in a chamber of cross section $a \times b = 6 \times 25$ mm^2; 12×25 — the same for a cross section $a \times b = 12 \times 25$ mm^2.

In this article the term cavitation hysteresis will refer to the delay in the onset of cavitation or the difference $\kappa^{\bullet} - \kappa^{\bullet}$ in the dependence $\kappa(\lambda_{1,2})$.

$$P = \frac{p - p_\infty}{\gamma q_n}, \qquad q_n = \frac{v_n^2}{2g} \cdot \frac{u_n^2}{2g}$$

$$R = \frac{u_r a_r}{\nu}, \qquad S = \frac{N a_r}{u_{rs}}, \qquad \varkappa = \frac{p_\infty - p_e}{\gamma q_n}$$

$$\lambda_1 = \frac{l_1}{a_r}, \qquad \lambda_2 = \frac{l_2}{a_r} \qquad\qquad (0.1)$$

$$\alpha = \frac{a_e}{a} = \alpha_1 \alpha_2, \quad \alpha_1 = \frac{a - a_r}{a}, \quad \alpha_2 = \frac{a_e}{a - a_r}$$

$$\alpha_c = \frac{a - a_c}{a - a_r}, \quad \alpha_{cr} = \frac{a - a_c}{a} = \alpha_1 \alpha_c$$
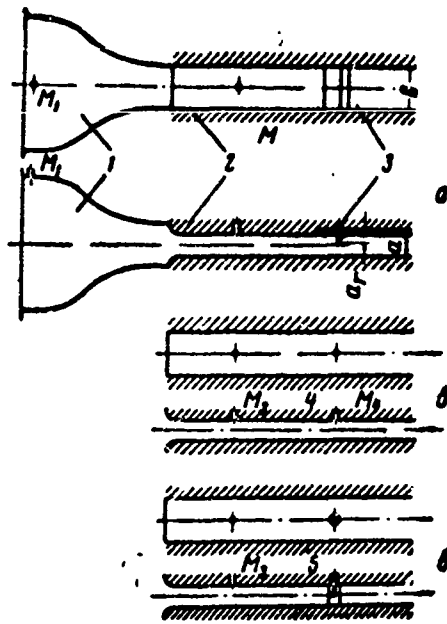
Fig. 1. Schematic of experiments with irregularity models in the GT-2: 1) nozzle, 2) working chamber, 3) model of irregularity, 4) nipple, 5) circular cylinder; a) schematic of basic experiments, b) schematic of pressure calibrator, c) schematic of velocity calibrator.

1. Description of experiments. Experiments with cavitation by a surface irregularity described below were carried out in the GT-2 hydrodynamic tube at the Institute of Mechanics, Academy of Sciences, USSR in a working chamber whose transverse section can be varied by the transposition of two oppositely located plexiglass walls. The irregularity models — right-angle prisms with cross section in the form of an isosceles right triangle — were prepared from rolled brass together with their base — plates set up in a depression of one of the plexiglass walls flush with the surface of the wall (Fig. 1, a; Table 1).

The experiments were divided into calibration and basic tests.

Table 1

a_p, mm	u_{2}	u_p m·sec^{-1}	$T,°C$	$R×10^{-4}$
Chamber $a×b=6×25$				
2.4	14.0	13.95	18.5	32.0
2.4	10.0	9.95	19.0	23.0
2.1	14.0	13.9	16.5	27.5
2.1	10.0	9.93	17.0	19.1
1.8	14.0	13.85	16.5	22.7
1.8	10.0	9.9	16.7	16.25
1.5	17.0	16.8	16.5	22.9
1.5	14.0	13.85	16.5	18.9
1.2	20.0	19.75	16.5	21.5
1.2	17.0	16.8	16.5	18.3
1.2	14.0	13.8	16.5	15.0
0.8	20.0	19.1	16.0	13.3
0.8	14.0	13.35	16.0	9.3
0.6	20.0	18.4	16.5	10.0
0.6	17.0	15.6	16.3	8.45
0.6	14.0	12.85	16.0	6.7
0.2	20.0	15.6	16.0	2.71
0.2	17.0	13.25	16.0	2.3
0.2	14.0	10.9	16.0	1.89
0.1	20.0	14.1	16.0	1.23
0.1	17.0	12.0	16.0	1.04
Chamber $a×b=12×25$				
4.8	14.0	14.0	18.0	63.3
4.8	10.0	10.0	19.0	46.4
4.2	14.0	14.0	17.0	54.0
4.2	10.0	10.0	17.0	38.7
3.0	17.0	17.0	16.0	44.3
3.0	14.0	14.0	16.5	38.4
3.0	10.0	10.0	17.5	28.1
2.4	14.0	13.96	18.5	32.0
2.4	17.0	16.9	18.5	38.8
2.1	20.0	19.8	18.0	39.2
2.1	17.0	16.25	19.0	34.2
2.1	14.0	13.9	19.5	28.6
1.8	20.0	19.7	18.0	33.5
1.8	17.0	16.75	18.5	28.8
1.8	14.0	13.8	19.0	24.0
1.5	20.0	19.6	19.5	28.8
1.5	17.0	16.65	20.0	24.8
1.5	14.0	13.7	20.0	20.3
1.2	20.0	19.3	17.5	21.7
1.2	17.0	16.4	18.0	18.5
1.2	14.0	13.5	18.5	15.5
0.8	20.0	18.6	29.0	14.7
0.8	17.0	15.8	19.5	12.4
0.8	14.0	13.0	20.0	10.3
0.6	20.0	17.8	18.0	10.1
0.6	17.0	15.1	18.0	8.55
0.6	14.0	12.45	18.5	7.15
0.2	20.0	15.2	17.0	2.8
0.2	17.0	12.9	17.5	2.41
0.2	14.0	10.6	18.0	2.0
0.1	20.0	13.8	17.0	1.27
0.1	17.0	11.7	17.5	1.09

Calibration tests had as their objection the determination of a connection between the magnitude of the velocity in·the measurement cross section where the model is located and the pressure at this point as a function of the pressure drop at the interval from the section M_1 of the nozzle inlet and up to the section M_3 in the working chamber.

Measurements of the pressure difference in sections M_1 and M_2 gave a small value for $p_1 - p_2$ and consequently the pressure p_2 was not subsequently used.

When carrying out experiments on tare pressure a nipple was mounted in the measurement cross section at point M_4 with its orifice flush with the surface of the chamber bottom (Fig. 1, b). While taking tare measurements of flow velocity a circular drained cylinder of $d = 6$ mm was mounted along the axis with the pressure outlet from pressure openings located along the vertical at different distances from the body outside of the manometer (Fig. 1, c). The cylinder was oriented so that the pressure openings were brought to the axial foward point of a cylinder $M_\bullet$ where the pressure must equal

$$\frac{p_c}{\gamma} = \frac{p_4}{\gamma} + \frac{v_n^2}{2g}$$

According to experiments in the absence of t ylinder was found the dependence (Fig. 2)

$$p_4 = f(p_1 - p_2) \qquad (1.1)$$

According to experiments with the cylinder at first was found the dependence

$$p_c = f(p_1 - p_2)$$

and then

$$|p_c - p_4| = f(p_1 - p_2) = q_n = \frac{v_n^2}{2g}$$

and the velocity

$$v_n = \sqrt{2gq_n} = f(p_1 - p_2) \qquad (1.2)$$

The difference $p_3 - p_4 = p_{3,4}$ is plotted (Fig. 2) for the determination of p_∞ .

In the formulas listed $\underline{n}$ is an index indicating to which point
of the measurement direction the velocity refers.

Using the cylinder the velocities were calibrated at a length
from the mean point of the cylinder height to a point located at
a distance y_1 = 1 mm from the chamber bottom.

In the boundary layer velocities were calculated from the
formula [12]

$$ u = u_1 \left(\frac{y}{y_1} \right)^{1/n} $$

Here u_1 is the velocity magnitude (Fig. 3) at a distance from
the wall of y_1 = 1.0 mm.

The basic experiments consisted of the fact that with a certain
constant velocity magnitude v_0 a change in pressure within the
tube produces different stages of cavitation determined visually
as a function of length of the cavitation zone. To determine the
moment of onset of cavitation a whole series of experiments at a
given velocity were carried out for a second time: at first the
pressure was gradually reduced (direct function) beginning from
complete absence cavitation right up to the development of the
separation stage of cavitation and then, repeating the experiment,
the pressure was increased beginning from the stage of separation
cavitation to complete suppression (inverse function). Here the
development of cavitation was determined according to the presence
of a characteristic noise and the simultaneous flickering "clouds"
— the cavitation cavern while the absence of cavitation is determined
from the secession of noise with the simultaneous secession of cavern
flickering.
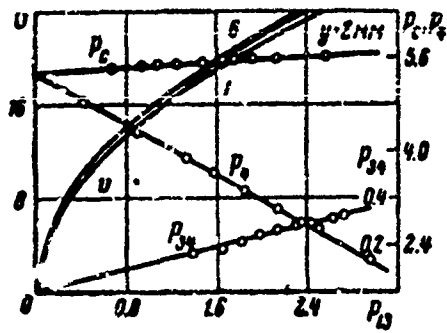
Fig. 2. Sample plot of a
calibration curve for the
variant 12 × 25.
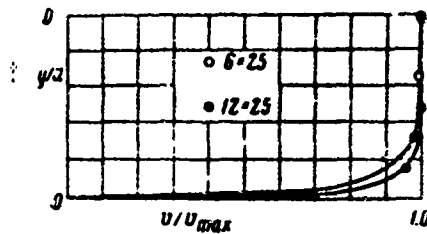
Fig. 3. Velocity curves
in the line of measure-
ment for two chamber
variants: 6 × 25 and
12 × 25.

At each stage of cavitation measurement was made of pressure at the point M_1 and M_3 (Fig. 1), water temperature T°C, barometric pressure, distance from the peak of the irregularity to the leading edge of cavitation zone l_1, the distance from the peak of the irregularity to the trailing edge of the cavitation l_2, the maximum height of the constraining cross section of the working chamber of the cavitation zone a_e reckoned from the bottom of the chamber. In passing the density of the cavitation zone and noise effects were noted.

The magnitude of pressure in the measurement cross section may be found by means a graph (Fig. 2) of the calibration function (1.1)

-9-

according to the formula

$$\frac{p_\infty}{\gamma} = \frac{\bar{p_4}}{\gamma} = \frac{p_3}{\gamma} - 10.33 |p_3 - p_4|$$

and the magnitude of velocity by means of the graph (Fig. 2) of the dependence (1.2).

The cavitation coefficient κ may then be calculated according to formula (0.1) where the water vapor pressure p_v was found from a table of physical constants as a function of temperature and q_n is calculated with respect to velocity at the level of the irregularity peak.

Experimental results were represented on the graphs $\kappa(\lambda_{1,2})$, $\kappa^\bullet$ and $\kappa^\bullet(a_r/a)$ where $\lambda_{1,2} = l_{1,2}/a_r$ and $\kappa^\bullet$ is the value of κ which corresponds to the onset of cavitation during the direct course of the experiments with a reduction in pressure and $\kappa^\bullet$ is the value of κ which corresponds to the suppression of cavitation in the inverse course of the experiments with an increase in pressure.

The curve of values K calculated according formula (2.5) also has an effect on the curves $\kappa^\bullet$ and $\kappa^\bullet$ (a_r/a).

In order to explain the kinematic structure of the cavitation zone high speed moving pictures were made of the cavitation zone for three experiment variations in the 12 × 25 chamber with the irregularities $a_r = 0.6$, 1.2 and 3.0 mm with $v_0 = 17$ msec^{-1}. For these experiments the SKS-1 movie apparatus was used permitting photographs at the rate of 8000 − 9000 frames·sec^{-1}. The apparatus was set so that its optical axis was dormal to the chamber bottom and the cavitation zone beyond the irregularity would be photographed in the plane. The photoscale was 1: 6.5.

2. <u>Consideration of experimental results.</u> In this section we

shall consider the following aspects of cavitation on a surface irregularity: 1) the external form of the cavitation zone and its kinematic structure; 2) the dependence $\kappa(l_{1,2})$; 3) the dependence κ° and $\kappa^{\bullet}(a_{r}/a)$ and the generalized formula of the dependence K on the geometric parameters of the flow and the relative height of the irregularity.

a. External form of the cavitation zone. According to visual observations there are two forms of cavitation behind a surface irregularity: 1) cavitation conditioned strictly by the irregularity model, and 2) cavitation conditioned by the finite nature of the length of the irregularity model or looseness of joining the front ends of the models to the chamber walls, — slot cavitation (Fig. 4). If experiments are carried out in a direct path then it may be noted that κ° and $\kappa^{\bullet}$ will differ for both forms of cavitation.
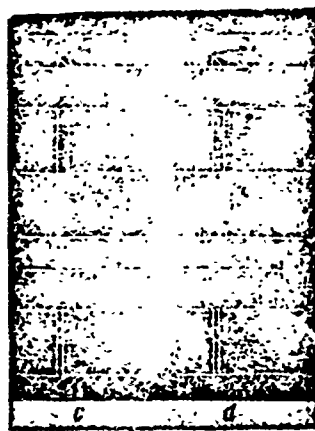
Fig. 4. Recordings of typical cavitation zones of two stages for two variants of irregularity model: $a_{r} > 0.9$ mm and $a_{r} < 0.9$ mm.

Here in experiments with a direct path with the variants $a_{r} \leqq$ $\leqq 0.9$ mm there arises at first an orifice cavitation and then

-11-

cavitation of the irregularities or $\kappa_{al}^{\bullet} > \kappa_r^{\circ}$ and with the variants $a_r \leqq 0.9$ mm there is at first observed cavitation of the irregularities or $\kappa_r^{\circ} > \kappa_{al}^{\bullet}$.

Comparison of the graphic representation of the dependence $\kappa(\lambda)$ made for various flow rates but for the same a_r makes it possible to evaluate the degree of similarity in the development of the cavitation zone as a function of R number. The same comparison made at identical flow velocities but for various variants of the working chamber and irregularities makes it possible to determine similar cavitations as a function of the size of the irregularity models.

Let us consider four dependences $\kappa(\lambda_1)$ common for all of the experiments. From a certain value of κ the magnitude of $\kappa \rightarrow$ const while $\lambda_1 \rightarrow \infty$ (Fig. 5). Such a form of $\kappa(\lambda_1)$ is explained by the positive pressure gradient [13] along the axis of the working chamber which for the 6×25 mm^2 chamber will equal

$$|p_3 - p_4|/(\gamma l_{3-4}) = 0.035$$

and for the 12×25 mm^2 chamber about 0.021. With a decrease in κ the magnitude λ_2 approaches $\lambda_2 = 0$ which indicates the approach of the cavitational zone to the peak of the irregularity.

The most important result of these observations consists of the fact that in the initial stage cavitation developes at some distance from the irregularity. With a reverse course of the experiment cavitation is reduced only at a certain length $\lambda_1 = 6 - 8$ independent of the flow of velocity or the height of the irregularity. The process of cavitation suppression was expressed in the fact that the cavitation zone having reached $\lambda_1 = 6 - 8$ gradually became less

dense at the surface and then vanished. Cavitation noise simultan-
eously changed or disappeared but it was not noted whether the
cavitation zone approached clear to the irregularity model.
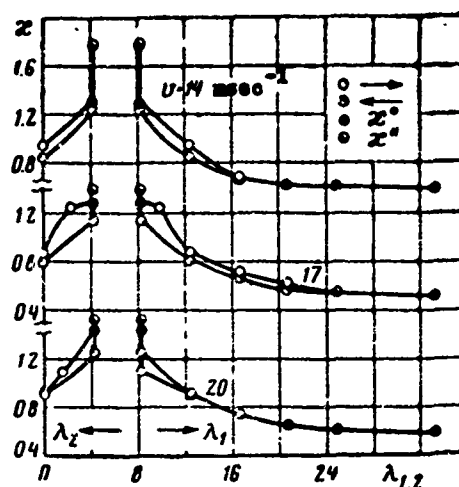
Fig. 5. Typical development
of the cavitation zone $\kappa(\lambda_2)$
in a 12 × 25 chamber behind
the model $a_r = 1.2$ mm.

The method of direct and reverse approach in carrying out the
experiments had the objective of determining the "hysteresis" of
the development of cavitation at its various stages.

In the general case the external appearance of hysteresis was
revealed by the fact that when the pressure is reduced in the
absence of cavitation in the first moments of the experiment cavita-
tion arises at a lower pressure than that at which it is suppressed
at higher pressures. When cavitation arises then its zone at once
takes on the form of a completely developed cavitation. As a result,
in the developed stages hysteresis was not as clearly detected as
might be asserted regarding its existence. In the initial stage,
namely at the moment of inception, various values of $\kappa^{\bullet}$ might be
obtained during the experiments depending upon how great the initial

-13-

pressure is in the tube before the moment of direct conduct of the experiment and what was the degree of pressure reduction. The greater the velocity the lower the difference between $\kappa^{\bullet}$ and κ^{o} but always $\kappa^{\bullet} > \kappa^{\bullet}$. On the sample graph of $\kappa(\lambda_{1.2})$ for the experiment variant 12 × 25, a_{r} = 1.2 mm, v_{0} = 14, 17 and 20 $msec^{-1}$ (Fig. 5) it is possible to note such a hysteresis "loop".

b. <u>Kinematic structure of the cavitation zone.</u> Experiments with high-speed movies were carried with a calculation so as to embrace cases when the peaks of the irregularities extend from the boundary layer, are completely submerged in the boundary layer and take a certain medium position. In Table 2 and in Fig. 6 are presented the results of experiments with irregularity models in the 12 × 25 working chamber at a velocity v_{0} = 17 $msec^{-1}$. It should be noted that N here designates the frequency of disruption of the cavern and the frequency of changes in the structure of the cavitation zone excited, of course, by pressure pulsations.

Table 2. (a-b — first digit —
— number of experiments, second —
— film number)

ab	$a_{r},\ мм$	a_{r}/a	λ_{2}	$\varkappa$	$N.\ ops$	s
1-5	0.6	0.05	10	0.7	500—1000	0.016—0.03
2-3	1.2	0.1	12.5	0.9	500—750	0.033—0.05
3-2	1.2	0.1	16.6	0.86	450—1500	0.03 —0.10
4-7	3.0	0.25	6	2.76	600—1100	0.05 —0.10
5-8	3.0	0.25	12	2.6	650—1000	0.05 —0.11

<u>Experiment 1-5.</u> The height of the irregularity model a_{r} = 0.6 mm, the actual length of the zone l_{2} = 6 mm. The irregularity is completely submerged in the boundary layer. On individual frames of the movie film the cavitation zone had the form of an accumulation

-14-
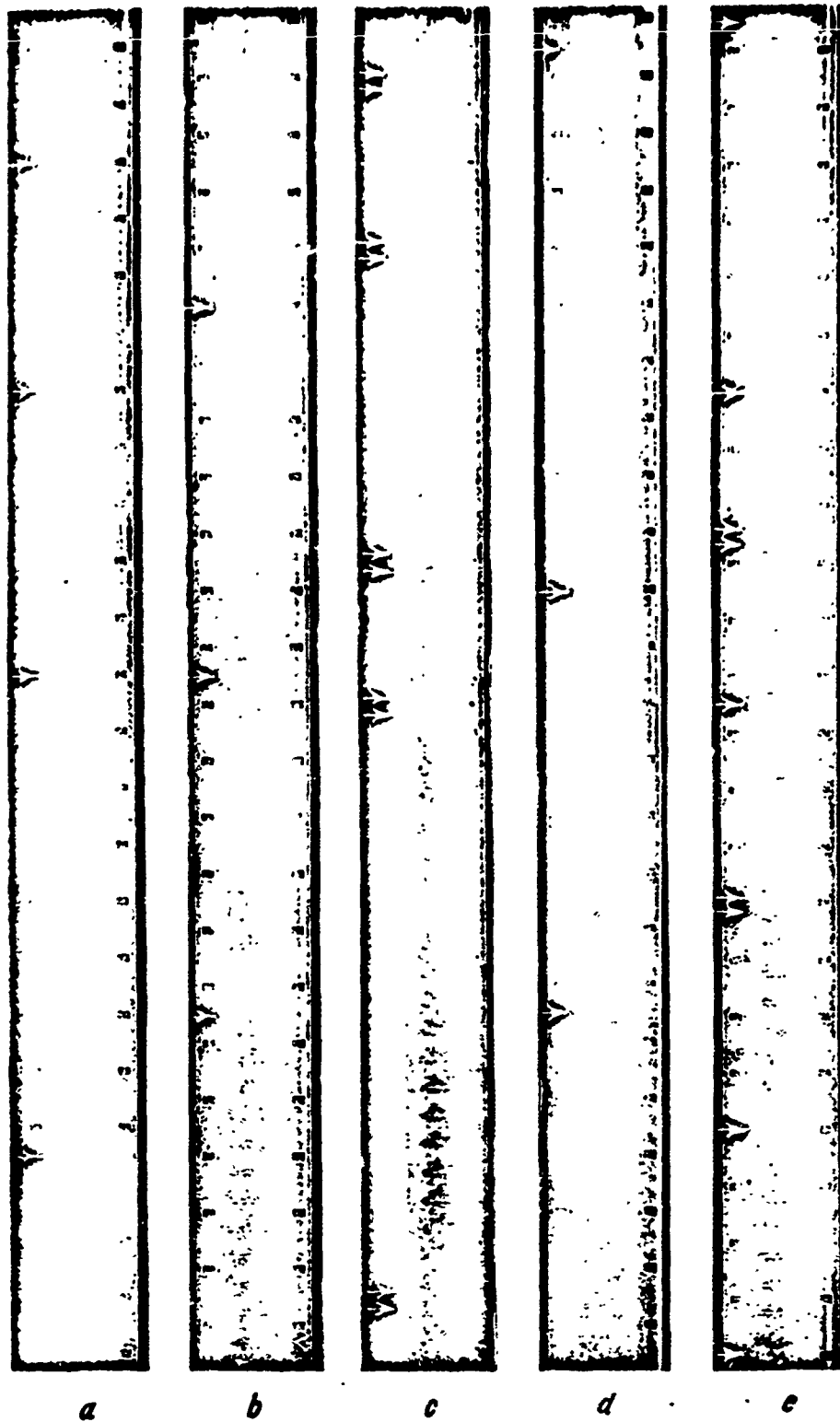
Fig. 6. Individual frames of a film of the cavitation
zone beyond an irregularity from an experiment in the
12×25 chamber taken at a frequency of $8000 - 9000$
frames·sec^{-1} with $v = 17$ msec^{-1}; data (Table 2):
a) experiment 1-5; b) experiment 2-3; c) experiment
3-2; d) experiment 4-7; e) experiment 5-8. Arrows
indicate identical stages of cavitation.

-15-

of individual caverns (or bubbles) of various form arranged beyond the irregularity on a strip 1 mm wide. The density of distribution of the caverns, their number and size varied in time with a period of 0.002 and 0.001 sec. During the extent of several intervals the appearance of individual fine caverns within the cavitation zone with a lifetime of 0.0005 sec is observed. Tracing the periodic nature of the appearance of caverns comprising the cavitation zone complicates the measurement of the zone itself or of pulsations in its volume. It may only be verified that the cavern during its development and motion does not leave the boundaries of the cavitation zone of maximum potential.

If the Strouhal number is taken into account for individual caverns having selected as the period of their emergence the duration of their development, we obtain $S = 0.08$.

Experiment 2-3. The height of the irregularity model $a_r = 1.2$ mm, the actual length of the cavitation zone equalled 18mm.

The peak of the irregularity was located at the edge of the boundary layer. On the frames of the movie film the cavitation zone was removed by no more than 3 mm from the irregularity. The cavitation zone consists of larger caverns than in experiment 1-5 but was also subject to periodic pulsations accompanied by breakdown of the caverns. At certain moments of the period a detachment from the tail of the cavitation zone of individual cavern is noted. They pertain to flows at a distance from the model equal to twice the length of the cavitation zone and are only there completely compressed. The periodic nature of the changes of the cavitation zone may be evaluated by the number $S = 0.033 - 0.050$.

Experiment 3-2. The height of the irregularity model $a_r = 1.2$ mm

-16-

as in the previous experiment but the length of the cavitation zone equalled 24 mm. Another difference from the preceding experiment is the fact that on frames of the movie film a periodic detachment of the cavern is clearly recorded with a period varying from 0.0022 to 0.00061 sec which gives a Strouhal number S = 0.03 – 0.1.

Experiment 4-7. The height of the irregularity model $a_p = 3$ mm, the length of the cavitation zone $l_2 = 18$ mm. On frames of the movie the cavitation zone appears as an accumulation of fine caverns of time-variable density. The period of pulsation of the zone varied over the range from 0.0017 to 0.001 sec. The departure of the cavern from the model proceeds no further than the cavitation zone. The Strouhal number varies within the limits S = 0.05 – 0.1.

Experiment 5-8. The model height equalled $a_p = 3$ mm, the length of the cavitation zone 35 mm. On frames of the movie film the cavitation zone consists of accumulations of caverns of variable density. In the intervals between decomposition of the caverns into fine caverns it is possible to see that the cavitation consists of extended spindle-shaped caverns with a number to three and with the long axis parallel to the axis of the irregularity. The period of pulsation of the zone amounts to 0.0015 sec, the period of formation and break-up of individual cavern equalls 0.001 sec, the Strouhal number for both changes S = 0.05 – 0.11.

As the result of considering experiments with movie pictures of the cavitation zone we arrive at the following conclusions.

The pulsating development of caverns proceeded in the experiments carried out under the influence of the following three factors.

1. Emergences of cavitation in the region a nucleus of vortices being striped from the irregularity with a frequency N.

-17-

2. Passages of pressure waves as the results of self oscillations of the fluid column in the working chamber with a cross section 12 × 25 and length $l = 0.3$ m, the wave frequency $N_1 = c/4l = 1170$ cps where $\underline{c}$ is the velocity of sound in water.

3. Passages of pressure waves as the result of self oscillation of the column fluid between the outlet from the nozzle and the outlet from the diffuser located beyond the working chamber of length $l_2 = 0.8$ m, the wave frequency $N_2 = c/4l_2 = 438$ cps.

The cause of excitation of pressure waves is all probability cavitation in the diffuser. Passage of the pressure waves had an effect on the development of the cavitation zone also in the case where the frequencies N_1, N_2 and N were close to each other and when they differed by a whole number of periods. Because of such over-lapping it was especially difficult to determine the Strouhal period in experiments 1-5 and 2-3. If attention is given to what has been said it may be seen that the development of caverns must proceed under the absence of interfering factors in particular the character-ized Strouhal number $S \approx 0.1$. The latter indicates that cavitation of irregularities of small height may serve as the source of sound with a basic tone of high frequency.

c. Generalized formula of the dependence $K(a_r/a)$. Flow around an irregularity on the wall of a chamber may be represented as flow-past with a large bending of the stream with the formation of flow tightening and vortices in the compression region. (Fig. 7, a). On the axis of rotation of the vortices cavitation with an appropriate reduction in pressure. Compression of the flow may be characterized by the coefficient of compression $\alpha = a_\bullet/s$. Total compression of

-18-

the flow behind the irregularity up to the onset of cavitation must
be comprised of compression of the flow by the irregularity $\alpha_1 = (a - a_r)/a$ and compression of the stream from the peak of the irregularity
$a_2 = a_3/(a - a_r)$.
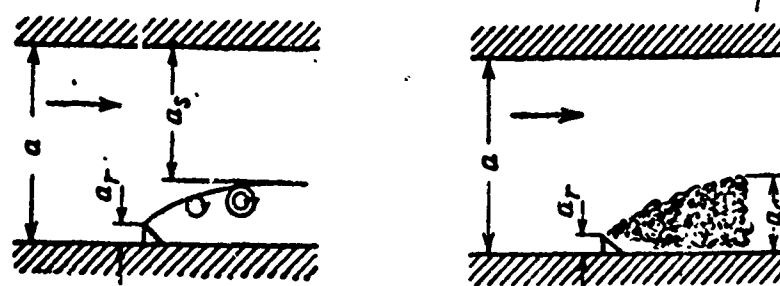
Fig. 7. Schematic of the flowpast of a model
irregularity of infinite prolongation in a
channel of finite height: a) without cavitation,
b) with cavitation.

Let us construct the Bernoulli equation from cross section
M_∞ (Fig. 7, a) to cross section M_a passing through the maximum
compression of the stream by the vortex

$$\frac{p_\infty}{\gamma} + \frac{v^2}{2g} = \frac{p_a}{\gamma} + \frac{v_a^2}{2g} + \zeta \frac{v^2}{2g} + \zeta_a \frac{v_a^2}{2g} \qquad (2.1)$$

where ζ is the coefficient of the sum of hydraulic resistances from
cross section M_∞ to the irregularity and ζ_a the coefficient of
resistance over stream compression by the irregularity, $\underline{v}$ the average
velocity at cross section M_∞. As has been pointed out above in the
description of the experiments the loss of energy to resistance from
M_∞ to the model is taken into account when determining p_∞. On this
basis it is possible to neglect the quantity $\zeta_1 v^2/2g$.

If we note that $v_a = v/\alpha$ then the pressure in the streams of
the compression cross section will equal

$$\frac{p_s}{\gamma} = \frac{p_\infty}{\gamma} + \frac{v^2}{2g} - \frac{v^2}{\alpha^2 2g} - \zeta_s \frac{v^2}{\alpha^2 2g} = \frac{p_\infty}{\gamma} - \frac{v^2}{2g}\left(\frac{1+\zeta_s}{\alpha^2} - 1\right) \qquad (2.2)$$

According to theoretical presentations concerning the structure of a turbulent cord [14] rotation of particles of the liquid within the turbulent cord proceeds with a constant angular velocity and the pressure on the axis of the vortex is expressed by the formula

$$\frac{p_0}{\gamma} = \frac{p_k}{\gamma} - \frac{v_k^2}{2g} \qquad (2.3)$$

where p_k and v_k are the pressure and velocity on the periphery of the vortex.

If we take $v_k = v_s$ and $p_k = p_s$ and replace p_s by its expression (2.2) then the pressure on the axis of the vortex, coinciding with the compression cross section, will equal

$$\frac{p_0}{\gamma} = \frac{p_\infty}{\gamma} - \left(\frac{2+\zeta_s}{\alpha^2} - 1\right)\frac{v^2}{2g}$$

For the moment of onset of cavitation it is necessary to set $p_0 = p_v$. After transferring terms we obtain

$$K = \frac{p_\infty - p_v}{\gamma q} = \frac{2+\zeta_s}{\alpha^2} - 1 \qquad (2.4)$$

for

$$K \approx \frac{2}{\alpha^2} - 1 \qquad (2.5)$$

i.e. an expression for the critical value of the coefficient of cavitation of the irregularity indicating its dependence on the geometric parameters of the irregularity α_1 and of the flow α_2 if one does not take into account the losses of energy to hydraulic resistance with compression of the stream, $\zeta_s = 0$.

If the height of the chamber or the thickness of the flow were to be increased or the height of the irregularity decreased, i.e.

$a_g/a \to 0$ and $\alpha \to 1$ then the value of K will tend toward $K = 1$.

For other ratios a_g/a it would be possible to calculate K, if it were possible to determine α_g theoretically, as the coefficient of compression of the stream during flow from opening with a sharp edge. Existing theoretical calculations of α proceed from the jet flowpast of the thin edge of an opening. Here consideration is not given to the circumstance that the arising eddy bends may somehow effect the degree of compression of the stream.

d. Comparison of theory with experiment. Expression (2.5) for the critical value of K was derived on the assumption that the velocity and pressure are distributed in the flow cross sections, excluding the vortex region, uniformly. Such an assumption is justified for those cases where the peaks of the irregularities project from the boundary layer. Otherwise the velocity of flowpast of the irregularity peaks may significantly differ from the velocity beyond the boundary layer and the question arises as to what velocity κ, obtained experimently, refers. In this article experimental values of κ refer to velocities in the boundary layer at the level of the irregularity peaks. Close coincidence of theoretical and experimental values of K and $\kappa^{\bullet}$, $\kappa^{\bullet}$ (Fig. 8, 9) is considered the criteria of validity of this assumption.

Another question which arises when considering the results of experiments refers to the selection of $\kappa^{\bullet}$ or $\kappa^{\bullet}$ for comparison with its theoretical value of K. The lowest values of $\kappa^{\bullet} < \kappa^{\epsilon}$ are explained, no doubt, by the fact the water in the tube before the start of the experiment is subject to a pressure which contributes to the diffusion of "nuclei" of cavitation. During the reverse course of the experiments the water in the tube is supersaturated

with cavitation nuclei. A higher pressure than the pressure during
the direct course of the experiments is required for the same flow
velocity in order to yield cavitation.
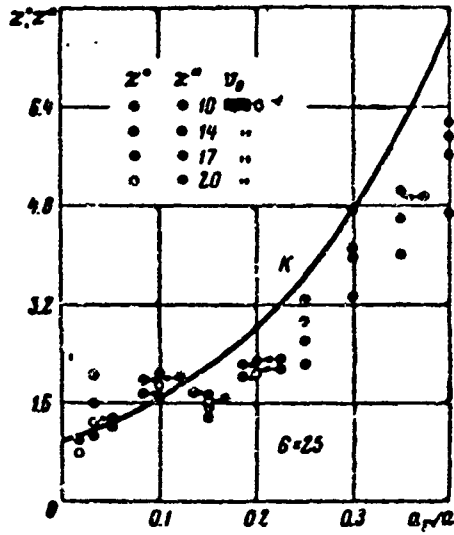
Fig. 8. Dependence of critical
values of κ^b, κ and K on relative
height of irregularities a_r/a for
the 6 × 25 variant of the working
chamber.
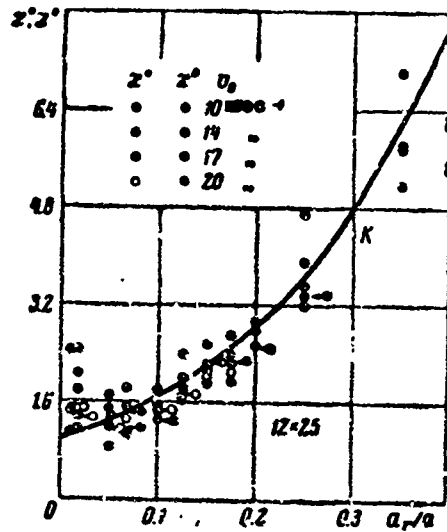
Fig. 9. Dependence of the magni-
tude of $\kappa^\bullet$, κ and K on the relative
height of the irregularity a_r/a for
the 12 × 25 variant of the working
chamber.

For the reasons given two groups of points $\kappa^{\bullet}$ and $\kappa^{\bullet}$ are plotted on the graphs of $\kappa^{\bullet}$ and $\kappa^{\bullet}$ (a_{r}/a) (Figs. 8 and 9). The theoretical curve $K(a_{r}/a)$ must pass between the experimental values of $\kappa^{\bullet}$ and $\kappa^{\bullet}$. This requirement is best satisfied by the experiments in the 12 × 25 chamber.

Let us consider in somewhat more detail this method of calculating the generalized dependence $K(a_{r}/a)$ according to formula (2.5). The most important effect on the magnitude of $\underline{k}$ is the coefficient of compression of the flow α. The coefficient α in turn depends on α_1 and α_2. The coefficient α_1 is given by the geometric parameters of the channel and of the irregularity. It is appropriate to make a number of observations with regard to the coefficient α_2.

V. A. Shaumyan [15] conducted numerous experiments on the direct determination of the coefficient of stream compression in the two cases: 1) with free flow from under a shield, i.e. the stream beyond the shield has a free unsubmerged level and 2) with sudden contraction of the stream upon passage of the flow from a wide channel to a narrow one, i.e. when the stream is submerged in the compression plane. In both cases the effect of preliminary compression coefficient was demonstrated. Moreover, it became clear that if the stream is not submerged in the compression plane then α_1 has a lower value than in the case when the stream is submerged. This apparently evidences the drawing under action of vortices which arise on both sides of the stream. The function α_2 (a_{r}/a) in this latter case if applicable to the experiment carried out, i.e. for values of $a_{r}/a =$ $= 0$ to 0.4 (Fig. 10), it may be represented thus:

$$\alpha_2 = 0.5\left(2 - \frac{a_r}{a}\right) \qquad (2.6)$$
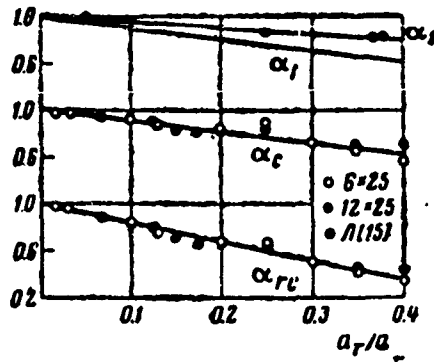
Fig. 10. Effect of relative
height of irregularity or
degree of preliminary com-
pression on the coefficients
α_1, α_2, α_e and α_{er}.

On the other hand we made an attempt to determine α_2 from

measurements of cavitation-zone flow compression. As can be seen

from a comparison of α_2 and α_e, determined by both methods (Fig. 10).

Compression of the cavitation-zone flow exceeds the compression

brought about by the compression of the flow and by vortex formation

in the absence of cavitation.

Keeping in mind all of the above remarks concerning the approach

to experimental determination of $\kappa^\bullet$, $\kappa^\bullet$ and the calculation of K

according to Eqs. (2.5) and (2.6), it is possible to explain the

divergence of experimental points and their deviation from the curve

K (a_r/a) in Figs. 8 and 9 by the following: 1) cavitation hysteresis;

2) the effect of flow velocity on hysteresis; 3) ambiguity in the

selection of the magnitude of velocity in the boundary layer to which

the critical value of κ must be referred; 4) a certain ambiguity in

the coefficients α_2 used for calculating the curve K (a_r/a). Large

values of experimental κ for a_r/a $\approx$ 0.05 (Figs. 8, 9) are explained

by the fact that slot cavitation is absent as was pointed out

earlier in § 2, a. Never the less, the "distribution" of most of

the experimental points to the theoretical curve provides a basis

-24-

for supposing a prpbability in the assumption made regarding the role of the vortex in the generation of cavitation. Consideration of the experimental results of Holl [8] leads to the same conclusion.

e. Comparison with the experiments of Holl. As was mentioned above, Holl studied the conditions of cavitation onset of irregularity models of two profile types: triangular and segmented. Experiments were carried under three different experimental conditions: 1) in a hydrodynamic tube of circular cross section with a diameter D = 38 in.; 2) the same with a diameter of 12 in.; 3) in a tube of rectangular cross section 5 × 20 in. Irregularity models were placed in the first two variants on platforms of thickness $\underline{t}$ placed in the mean longitudinal cross section of the working chamber of the hydrodynamic tubes.

In variant I the irregularity models were placed in the middle portion of the plate width, their relative length being varied over the range l/a_p = 52 to 96. In variant II the irregularity models overlapped the plate width. Experimental results of variant III are not considered, this data being close to the data of variant II. The end of the irregularity models were cut obliquely so as to avoid cavitation in the flow passing the model on the surface. The dimensions of the test irregularities and the experimental results are given in Tables 3 and 4 where σ_i designates critical values of κ given by Holl. The values of σ_i correspond to suppressed cavitation and are referred to the velocity at the edge of the boundary layer, i.e. to $\underline{v}$. They are taken from the graph $\sigma_i = (a_p/\delta)$ where δ is the thickness of the boundary layer in inches, according to two curves corresponding v = 40 and 60 ft sec^{-1}. Magnitudes of κ_p were obtained by conversion of ξ_i according to the formula

$$x_r^{\bullet} = \frac{\sigma_i}{(u_r/v)^3}, \qquad \frac{u_r}{v} = \left(\frac{a_r}{\delta}\right)^n \qquad \left(n = \frac{1}{m} = \frac{1}{6} + \frac{1}{5.25}\right)$$

Table 3

a_r, inches	σ_i		$x_r^{\bullet}$		$\dfrac{2a_r}{D-i}$
	from	to	from	to	
Variant I, $\delta = 0.453$					
1/2	1.77	1.85	1.71	1.79	0.021
1/4	1.40	1.41	1.71	1.72	0.011
1/16	0.85	0.77	1.65	1.50	0.003
Variant II, $\delta = 0.293$					
1/16	0.93	0.89	1.56	1.49	0.011
1/40	0.71	0.66	1.61	1.50	0.004
1/100	0.44	0.38	1.36	1.17	0.002
4/1000	0.31	0.30	1.28	1.25	0.001
Variant I, $\delta = 0.117$					
1/2	2.05	2.20	1.28	1.35	0.021
1/4	1.57	1.52	1.27	1.23	0.011
1/16	0.94	0.88	1.32	1.24	0.003
Variant II, $\delta = 0.1197$					
1/16	1.03	0.97	1.32	1.24	0.011
1/40	0.80	0.75	1.52	1.42	0.004
1/100	0.55	0.49	1.41	1.26	0.002
4/1000	0.39	0.36	1.41	1.28	0.001

Table 4

a_r, inches	σ_i		$x_r^{\bullet}$		$\dfrac{2a_r}{D-i}$
	from	to	from	to	
Variant I, $\delta = 0.453$					
1/2	0.83	0.81	0.803	0.785	0.021
1/4	0.74	0.72	0.896	0.88	0.011
1/16	0.52	0.47	1.01	0.91	0.003
Variant II, $\delta = 0.293$					
1/16	0.54	0.47	0.906	0.79	0.011
1/25	0.48	0.40	0.92	0.78	0.007
1/40	0.41	0.36	0.93	0.82	0.004
1/100	0.31	0.306	0.96	0.95	0.002

Values of $\underline{n}$ given in parenthesis pertained to Holl.

It should be noted that values of σ_i for model of a segmented profile determined by acoustic and visual methods, were close to each other; for models of triangular profile the acoustic method gave lower values of σ_i. In this work the given σ_i were determined by the visual method.

Consideration of Table 3 where values of σ_i are given for models of triangular profile and Table 4 where values of σ_i are given for models of segemented profile leads to the following conclusions.

1. Values of σ_i referred to u_p for $a_p/a \approx 0$ do not depend on a_p/a for both model types which agrees with the conclusions of the work considered and earlier work [7] regarding the fact that when $a_p/a \to 0$ then the quantities $\kappa^{\bullet\bullet} \to$ const $= 1$.

2. Values of σ_i for segmented profiles for $a_p/a \to 1$ are closer to the theoretical $K = 1$ than σ_i for a triangular profile due to the presence in the method of experimental determination of the onset of cavitation (visual determination of σ_i with respect to suppressed cavitation for models of a triangular profile).

3. The same must be said when comparing σ_i with $\kappa_p^{\bullet}$.

3. __Regarding practical application.__ It has been pointed out earlier [7] that cavitation on a model of winged profile having an isolated irregularity on the surface arises at a higher value of κ_{pr} than on a smooth model. Let us consider this problem in the light of new data especially when $\kappa_p^{\bullet}$ is referred to the velocity u_p.

For a wing of flowpast profile with a smooth surface it is possible to write

$$\frac{p_\infty}{\gamma} + \frac{v_\infty^2}{2g} = \frac{p}{\gamma} + \frac{v^2}{2g} \qquad (3.1)$$

where p_∞ and v_∞ refer to flow in front of the wing at the point M_∞ while p and v refer to flow on the wing at the point M. Using the designation for velocity head $q = v^2/2g$ and joining to both parts of 3.1 the quantity p_v/γ, we obtain

$$\frac{p_\infty}{\gamma} - \frac{p_v}{\gamma} + q_\infty = \frac{p}{\gamma} - \frac{p_v}{\gamma} + q$$

-27-

or, introducing the quantities

$$\varkappa_{pr} = \frac{p_\infty - p_v}{\gamma q_\infty}, \qquad \varkappa_r = \frac{p - p_v}{\gamma q_r}, \qquad q_\infty = \frac{v_\infty^2}{2g}, \qquad q_r = \frac{u_r^2}{2g}$$

we obtain

$$\frac{\varkappa_\infty}{q_r} + \frac{1}{q_r} = \frac{\varkappa_r}{q_\infty} + \frac{q}{q_\infty q_r} = \varkappa_r \frac{q_r}{q_\infty} - 1 + \frac{q}{q_\infty} \qquad (3.2)$$

Designating the coefficient of pressure for a smooth wing by P

$$P = \frac{p - p_\infty}{\gamma q_\infty} = 1 - \frac{q}{q_\infty}, \qquad \frac{q}{q_\infty} = 1 - P$$

and replacing the quantity q/q_∞ by P in (3.2) we obtain

$$\varkappa_{pr} = \varkappa_r \frac{q_r}{q_\infty} - 1 + 1 - P = \varkappa_r \frac{q_r}{q_\infty} - P \qquad (3.3)$$

If at point M there is a minimum pressure P_{min} then on the basis
of the equality $\overset{\bullet}{\kappa_{pr}} = - P_{min}$ (condition of onset of cavitation of a
smooth-flowpast even wing) we will have $\kappa_r = 0$.

Such a value of κ_r indicates that the cavitation of the
irregularity will be located in the boundary stage of its development
independent of what level from the wing surface the peak of the
irregularity is located: within the boundary layer or beyond it.
At the same time the profile cavitation of a smooth wing will be in
the initial stage.

If the irregularity is situated outside the portion of the wing
surface having P_{min} and its peak extends beyond the boundary layer
then in (3.3) it is necessary to set $q_r = q$ and, having expressed
q/q_∞ in terms of P, we obtain

$$\varkappa_{pr} = \varkappa_r (1 - P) - P \qquad (3.4)$$

an expression given in a previous article [7] and then Holl [8].

At the point on the wing where P = 0 we have, from (3.4), $\kappa_{pr}^{\bullet} = \kappa_{p}^{\bullet} = 1$; then, as in the case of a smooth wing, cavitation will arise only for $\kappa_{pr}^{\bullet} = -P_{min}$.

If the height of the irregularity is sufficiently small it is possible to take $u_{p} = 0$, $q_{p} = 0$, then from (3.3) we will have

$$\varkappa_{pr} = -P = -P_{min}$$

or the onset of cavitation of a smooth wing.

Conclusion. 1. Cavitation of a surface irregularity in the initial stages developes in a zone of free vortices formed beyond the irregularity. The genesis of cavitation proceeds on the axis of the vortices.

2. The greatest danger with regard to the onset of cavitation are irregularities in narrow channels or slots where irregularities small in absolute dimension will be relatively large since K has a second-power dependence on the magnitude of crowding in the slit of the irregularity.

3. Experimental values of $\kappa^{\bullet}$ and $\kappa^{\bullet}$ tend, with a decrease in the relative irregularity height, to some limiting value, namely to K = = 1.0 in the case where $\kappa^{\bullet}$ and $\kappa^{\bullet}$ refer to velocities at the level of the irregularity peaks.

4. Attention should be given to the smoothness of the surface finish of those parts of hydromachines and hydrostructures which must operate under cavitation conditions, expecially those surfaces which form slots, for example the walls of wheel chambers of axial turbines and pumps, apposed faces of vanes, the surface of the spillway of concrete dams. If on the surface of some part there are formed surface irregularities similar to those studied, for example, groves, scratches, etc., it is necessary to check the possibility of

FTD-TT-65-1606/1+2+4

their cavitation with the use of values for K given in Fig. 8 or

to calculate K according to Eqs. (2.4) and (2.5).

REFERENCES

1. O. Silberrad. The Erosion of Bronzs Propellers. Journal Soc. Chem. Industr., vol. 40, No. 4, 1921.

2. H. O. Dahl. Kovitation vid Vattenturbiner. Kavitations — — Problemet. Ingeïörsvetenskapsakad. Medaelande. Stockholm, No. 112, 1938.

3. H. J. Petersen and J. E. Roberts. Hydraulic — Turbine Practice of the T. V. A. Mechanical Engng., vol. 65, No. 4, 1943.

4. K. K. Shal'nev. Opyt obsledovaniya kavitatsionnoy erozii turbii i nasosov bol'shchoy moshchnosti. Inkh. sb., t. 18, 1954.

5. H. Schröter. Korrosion bei Kavitation — Bericht über Versuche am Walchenseekraftwerk. Z. Ver. Dtscn. Ing., vol. 77, No. 32, 1933.

6. K. K. Shal'nev. Kavitatsiya nerovnostey poverkhnosti, ZhTF, t. 21, vyp. 2, 1951.

7. K. K. Shal'nev. Kavitatsiya nerovnostey poverkhnosti i vyzyvaemaya eyu eroziya. DAN SSSR, t. 78, No. 1, 1951.

8. J. W. Holl. The Inception of Cavitation on Isolated Surface Irregularitions. Trans. ASME, ser. D, J. Basic Engng. (Paper No. 59 — —Hyd.— 12), vol. 82, No. 1, 1960.

9. G. L. Calehuff and G. F. Wislicenus. ORL Investigations of Scale Effects on Hydrofoil Cavitation TM 19. 4212-03, Ordnance Research Laboratory, The Pennsylvania State University, February, 1956.

10. G. K. Walker Jr. Rotational Flow Over a Surface Protrusion. Master of Science Dissertation, Department of Aeronautical Engineering, The Pennsylvania State University, Jan., 1957.

11. D. Colgate. Cavitation Damage of Roughened Concrete Surfaces. J. Hydraulics Div., Proc. Amer. Soc. Civil Engrs., vol. 85, No. 11, 1959.

12. L. M. Prandtl'. Gidroaeromekhanika. M., Gostekhizdat, 1949.

13. K. K. Shal'nev. Vliyaniye gradiyenta·davleniya v potoke na razvitiye zony kavitatsii. PMTF, No. 1, 1961.

14. A. A. Catkevich. Ob osnovakh gidrodinamicheskoy teorii vikhrya. Tr. Nauchissled. aeroin-ta Ucheb. kombinata grazhd. vozdushn.

flota. L., St. 19, 1932.

15. <u>V. A. Shaumyan.</u> Teoriya shchitovykh vodomerov-regulyatorov
i ee prakticheskoye primeneniye v oroshenii. Tr. Vsesoyuzn. nauchn.-
issled. in-ta gidrotekhn. i meliorats., t. 22, 1938.